Recent Status of Lattice QCD for Muon g-2 and Electroweak Physics

Kohtaroh Miura
(KEK-IPNS, Theory Center)

PPP2023
August 31, 2023

Muon Anomarous Magnetic Moment

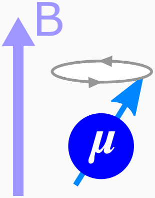

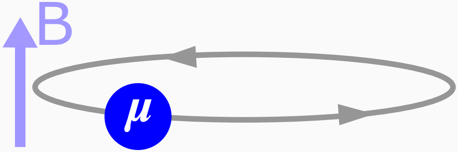

$\vec{\omega}_{spin}$ $\vec{\omega}_{cyc}$

- **Anomaly:**

$$\vec{\omega}_a = \vec{\omega}_{spin} - \vec{\omega}_{cyc} = a_\mu \frac{e\vec{B}}{m_\mu c} \,, \quad a_\mu = \frac{g_\mu - 2}{2} \,. \tag{1}$$

- **Pauli Eq.:**

$$i\hbar \frac{\partial \phi}{\partial t} = \left[\frac{(-i\hbar c\vec{\nabla} - e\vec{A})^2}{2m_\mu c} - \vec{M}_\mu \cdot \vec{B} + eA_0 \right] \phi \,, \quad \vec{M}_\mu = g_\mu \frac{e}{2m_\mu c} \frac{\hbar \vec{\sigma}}{2} \,. \tag{2}$$

Muon Anomarous Magnetic Moment in QFT

Dirac Theory

$$\vec{\omega}_a = \vec{0}\ ,\ a_\mu = 0\ ,\ g_\mu = 2\ .$$

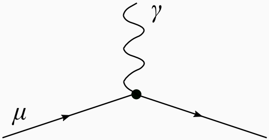

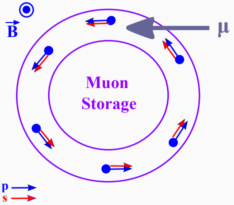

Quantum Field Theory (QFT)

$$\vec{\omega}_a \neq \vec{0}\ ,\ a_\mu > 0\ ,\ g_\mu > 2\ .$$

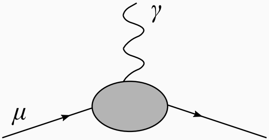

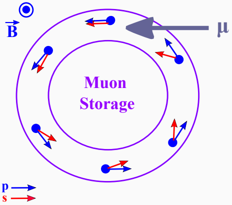

FNAL-E989 Arrival-Time Spectrum

Model function for positron energy spectrum:

$$N_{e^+}(t, E_{th}) = N_0(E_{th}) e^{-t/(\gamma\tau_\mu)} \left(1 + A(E_{th}) \cos[\omega_a t + \phi(E_{th})]\right) . \tag{3}$$

fitted to data about $600\mu s \sim 10\gamma\tau_\mu$.

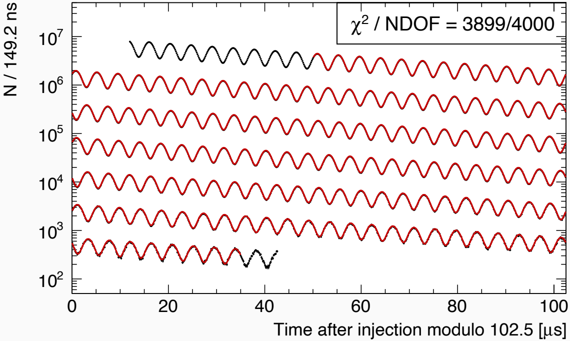

Figure: Quoted From FNAL-E989 Paper: PRD2021.

- **QFT Def. for Lepton g-2:**

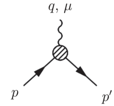

$$= \quad \langle \bar{\ell}^-(p)|\mathcal{J}^\mu|\ell^-(p')\rangle = \bar{u}(p)\Gamma^\mu(p,p')u(p')$$

$$\Gamma^\mu(q=p-p') = \gamma^\mu F_1(q^2) + \frac{i\sigma^{\mu\nu}q_\nu}{2m_\mu}F_2(q^2) + \cdots \, ,$$

$$F_2(0) = a_\ell = (g_\ell - 2)/2 \, .$$

- **Standard Model, Loop Corr.:**

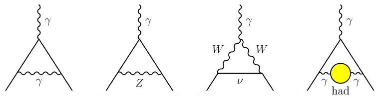

$$a_\ell^{1L\text{-QED}} = \frac{\alpha}{\pi}\int dQ^2\omega\left(\frac{Q^2}{m_\ell^2}\right) = \frac{\alpha}{2\pi} \, ,$$

$$a_\ell^{\text{LO-HVP}} = \left(\frac{\alpha}{\pi}\right)^2\int dQ^2\omega\left(\frac{Q^2}{m_\ell^2}\right)\hat{\Pi}_{had}(Q^2) \, .$$

- **BSM = SUSY (J. Ellis et al.'82) or Walking-TC (e.g. Kurachi et al. '13) or $\cdots$:**

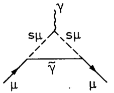

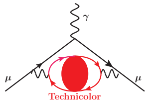

$$\propto (m_\ell/\Lambda_{BSM})^2 .$$

FNAL-E989 RUN-III (Aug. 10, 2023)

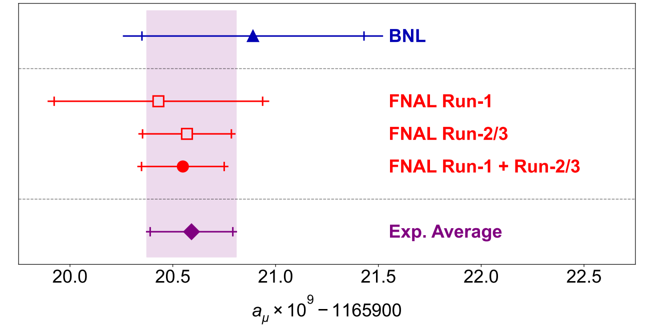

Figure: Quoted from FNAL-E989 RUN-III arXiv:2308.06230.

- RUN123: 0.2 ppm, RUN123 + BNL: 0.19 ppm, c.f. Goal: 0.14 ppm.
- 4-times statistics than RUN1 (2021). Homogeneous magnetic fields for the muon storage, even further than the original goal.

$a_\mu^{exp.}$ vs. a_μ^{SM}

SM contribution	$a_\mu^{\text{contrib.}} \times 10^{10}$	Ref.
QED [5 loops]	11658471.8931 ± 0.0104	[Aoyama et al '19]
Weak (2 loops)	15.36 ± 0.10	[Gnendiger et al '13]
LO-HVP($\mathcal{O}(\alpha^2)$) pheno.	693.1 ± 4.0	[White Paper '20]
NLO-HVP($\mathcal{O}(\alpha^3)$) pheno.	-9.84 ± 0.09	[Kurz et al '14, Jegerlehner '16]
	-9.83 ± 0.04	[KNT19]
NNLO-HVP($\mathcal{O}(\alpha^4)$) pheno.	1.24 ± 0.01	[Kurz et al '14]
HLbyL($\mathcal{O}(\alpha^3)$)	10.5 ± 2.6	[Prades et al '09]
Standard Model	11659181.0 ± 4.3 [0.37 *ppm*]	[White Paper '20]
Experiments	11659205.9 ± 2.2 [0.19 *ppm*]	[FNAL2023/BNL Aver.]
Exp. – SM.	24.9 ± 4.9 [5.1σ]	[FNAL2023/BNL - WP]

$$a_\mu^{\text{LO-HVP}}|_{NoNewPhys} = a_\mu^{\text{ex.}} - (a_\mu^{\text{QED}} + a_\mu^{\text{EW}} + a_\mu^{\text{(N)NLO-HVP}} + a_\mu^{\text{HLbL}}) \simeq (718.0 \pm 2.8) \times 10^{-10} \,.$$

Budget

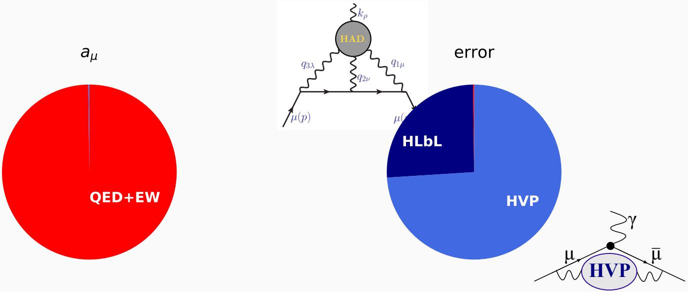

For 0.1ppm in total a_μ

- **HVP:** 0.2% precision. Challenging in LO-HVP. Tension in Pheno/LQCD?
- **HLbL:** 10% precision. Already achieved. No Tension in Pheno and LQCD.

THIS TALK

- **HVP Corrections to Running Coupling** $\hat{\Pi}(-Q^2) \propto \Delta\alpha_{\rm had}(-Q^2)$

- **LO-HVP Contributions to Muon g-2** $a_\mu^{\text{LO-HVP}}$

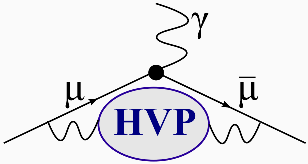

- **THIS TALK:**
  LQCD vs. Data-Driven (vs. Experiments) for $\Delta\alpha_{\rm had}(-Q^2)$ & $a_\mu^{\text{LO-HVP}}$.

Status Summary

- Experiments:
  - BNL-E821 (2004).
  - FNAL-E989: RUN1 (2021) & RUN3 (Aug. 10, 2023).
  - J-PARC-E34: Ultra-Cold Muon Beam. From the end of 2024?
- Data-Driven Phenomenology:
  - Theory Initiative White-Paper (Phys. Rep. 2020).
  - CMD3 Experiments for R-ratio (Feb. 2023).
- Lattice QCD (LQCD):
  - Theory Initiative White-Paper (Phys. Rep. 2020).
  - BMW-2020 (Nature-2021) c.f. PPP2020
  - Window Method (2022 - 23) & QED Running Coupling (2022).

Table of Contents

Table of Contents

Hadron Vacuum Polarization (HVP)

We need to evaluate Hadron Vacuum Polarization (HVP) non-perturbatively.

$$= \Pi_{\mu\nu}(q^2) = (q_\mu q_\nu - \eta_{\mu\nu} q^2)\Pi(q^2)\ .$$

Optical Theorem

$$\mathrm{Im}\Pi(s) = \frac{R(s)}{12\pi}\ , \quad R(s) := \frac{\sigma(e^+e^- \to \gamma^* \to \mathrm{had})}{4\pi\alpha^2(s)/(3s)}\ .$$

Optical Theorem

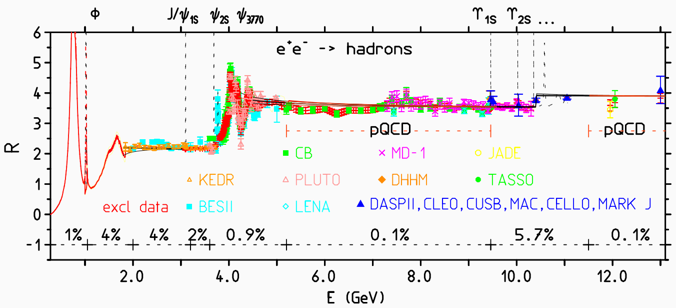

Figure: R-ratio quoted from Fig. 29 in White Paper (Phys. Rep. 2020).

$$\mathrm{Im}\Pi(s) = \frac{R(s)}{12\pi}\,, \quad R(s) := \frac{\sigma(e^+e^- \to \gamma^* \to \text{had})}{4\pi\alpha^2(s)/(3s)}\,.$$

Dispersion Relation

$$\hat{\Pi}(q^2) = \int_0^\infty ds \frac{-q^2}{s(s-q^2)} \frac{\mathrm{Im}\Pi(s)}{\pi} \quad \text{(dispersion)} ,$$

$$= \frac{-q^2}{12\pi^2} \int_0^\infty ds \frac{R(s)}{s(s-q^2)} \quad \text{(optical)} . \tag{4}$$

Dispersion Relation

We shall consider the function proportional to the real part of HVP:

$$F(q^2) \propto \hat{\Pi}(q^2) = \mathrm{Re}[\Pi(q^2) - \Pi(0)]\ . \tag{5}$$

Unitarity relates the real and imaginary parts:

$$F(q^2 \in \mathbb{R}) = \oint_{L+C+\bar{L}} \frac{dz}{2\pi i}\,\frac{F(z)}{z-q^2} \quad \text{(Cauchy)}$$

$$= \int_{L+\bar{L}} \frac{dz}{2\pi i}\,\frac{F(z)}{z-q^2} \quad \text{(integrand vanish at } C\text{)}$$

$$= \mathcal{P}\int_{4M_\pi^2}^{\infty} \frac{ds}{2\pi i}\,\frac{F(s+i\epsilon)-F(s-i\epsilon)}{s-q^2}$$

$$= \mathcal{P}\int_{4M_\pi^2}^{\infty} \frac{ds}{2\pi i}\,\frac{2i\,\mathrm{Im}F(s)}{s-q^2} = \mathcal{P}\int_{4M_\pi^2}^{\infty} \frac{ds}{\pi}\,\frac{\mathrm{Im}F(s)}{s-q^2}\ .$$

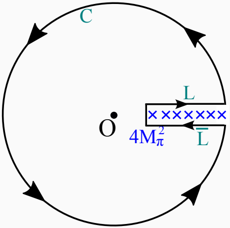

Naive identi $F(q^2) = \hat{\Pi}(q^2)$ does not work because $\mathrm{Im}\Pi(s \to \infty) = const$ results in a divergent integral.

Dispersion Relation

We shall consider the function proportional to the real part of HVP:

$$F(q^2) \propto \hat{\Pi}(q^2) = \mathrm{Re}[\Pi(q^2) - \Pi(0)] \,. \tag{5}$$

Unitarity relates the real and imaginary parts:

$$F(q^2 \in \mathbb{R}) = \oint_{L+C+\bar{L}} \frac{dz}{2\pi i} \frac{F(z)}{z - q^2} \quad \text{(Cauchy)}$$

$$= \int_{L+\bar{L}} \frac{dz}{2\pi i} \frac{F(z)}{z-q^2} \quad \text{(integrand vanish at } C\text{)}$$

$$= \mathcal{P} \int_{4M_\pi^2}^{\infty} \frac{ds}{2\pi i} \frac{F(s+i\epsilon)-F(s-i\epsilon)}{s-q^2}$$

$$= \mathcal{P} \int_{4M_\pi^2}^{\infty} \frac{ds}{2\pi i} \frac{2i\,\mathrm{Im}F(s)}{s-q^2} = \mathcal{P} \int_{4M_\pi^2}^{\infty} \frac{ds}{\pi} \frac{\mathrm{Im}F(s)}{s-q^2} \,.$$

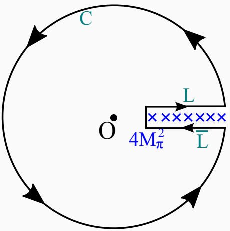

Naive identi $F(q^2) = \hat{\Pi}(q^2)$ does not work because $\mathrm{Im}\Pi(s \to \infty) = const$ results in a divergent integral.

Dispersion Relation

We shall consider the function proportional to the real part of HVP:

$$F(q^2) \propto \hat{\Pi}(q^2) = \mathrm{Re}[\Pi(q^2) - \Pi(0)] \ . \tag{5}$$

Unitarity relates the real and imaginary parts:

$$F(q^2 \in \mathbb{R}) = \oint_{L+C+\bar{L}} \frac{dz}{2\pi i} \frac{F(z)}{z - q^2} \quad \text{(Cauchy)}$$

$$= \int_{L+\bar{L}} \frac{dz}{2\pi i} \frac{F(z)}{z-q^2} \quad \text{(integrand vanish at } C\text{)}$$

$$= \mathcal{P} \int_{4M_\pi^2}^{\infty} \frac{ds}{2\pi i} \frac{F(s+i\epsilon)-F(s-i\epsilon)}{s-q^2}$$

$$= \mathcal{P} \int_{4M_\pi^2}^{\infty} \frac{ds}{2\pi i} \frac{2i\ \mathrm{Im}F(s)}{s-q^2} = \mathcal{P} \int_{4M_\pi^2}^{\infty} \frac{ds}{\pi} \frac{\mathrm{Im}F(s)}{s-q^2} \ .$$

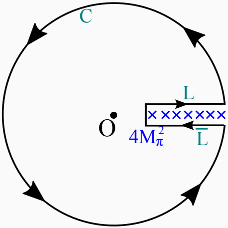

Naive identi $F(q^2) = \hat{\Pi}(q^2)$ does not work because $\mathrm{Im}\Pi(s \to \infty) = const$ results in a divergent integral.

Dispersion Relation

We shall consider the function proportional to the real part of HVP:

$$F(q^2) \propto \hat{\Pi}(q^2) = \mathrm{Re}[\Pi(q^2) - \Pi(0)] \,. \tag{5}$$

Unitarity relates the real and imaginary parts:

$$\begin{aligned}
F(q^2 \in \mathbb{R}) &= \oint_{L+C+\bar{L}} \frac{dz}{2\pi i}\, \frac{F(z)}{z-q^2} \quad \text{(Cauchy)} \\
&= \int_{L+\bar{L}} \frac{dz}{2\pi i}\, \frac{F(z)}{z-q^2} \quad \text{(integrand vanish at } C\text{)} \\
&= \mathcal{P}\int_{4M_\pi^2}^{\infty} \frac{ds}{2\pi i}\, \frac{F(s+i\epsilon)-F(s-i\epsilon)}{s-q^2} \\
&= \mathcal{P}\int_{4M_\pi^2}^{\infty} \frac{ds}{2\pi i}\, \frac{2i\,\mathrm{Im}F(s)}{s-q^2} = \mathcal{P}\int_{4M_\pi^2}^{\infty} \frac{ds}{\pi}\, \frac{\mathrm{Im}F(s)}{s-q^2} \,.
\end{aligned}$$

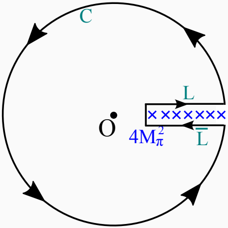

Naive identi $F(q^2) = \hat{\Pi}(q^2)$ does not work because $\mathrm{Im}\Pi(s\to\infty) = const$ results in a divergent integral.

Dispersion Relation

We shall consider the function proportional to the real part of HVP:

$$F(q^2) \propto \hat{\Pi}(q^2) = \mathrm{Re}[\Pi(q^2) - \Pi(0)] \,. \tag{6}$$

Unitarity relates the real and imaginary parts:

$$F(q^2 \in \mathbb{R}) = \oint_{L+C+\bar{L}} \frac{dz}{2\pi i}\,\frac{F(z)}{z-q^2} \quad \text{(Cauchy)}$$

$$= \int_{L+\bar{L}} \frac{dz}{2\pi i}\,\frac{F(z)}{z-q^2} \quad \text{(integrand vanish at } C\text{)}$$

$$= \mathcal{P}\int_{4M_\pi^2}^{\infty} \frac{ds}{2\pi i}\,\frac{F(s+i\epsilon)-F(s-i\epsilon)}{s-q^2}$$

$$= \mathcal{P}\int_{4M_\pi^2}^{\infty} \frac{ds}{2\pi i}\,\frac{2i\,\mathrm{Im}F(s)}{s-q^2} = \mathcal{P}\int_{4M_\pi^2}^{\infty} \frac{ds}{\pi}\,\frac{\mathrm{Im}F(s)}{s-q^2} \,.$$

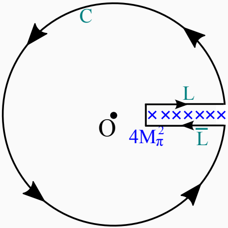

The correct identification is the once subtracted dispersion relation:

$$F(q^2) \equiv \frac{\hat{\Pi}(q^2)}{q^2} = \mathcal{P}\int_{4M_\pi^2}^{\infty} \frac{ds}{\pi}\,\frac{\mathrm{Im}\Pi(s)}{s(s-q^2)} \,.$$

The integral is finite. ($F(0) = const$ owing to the vector-current conservation.)

White Paper

In summary, the HVP is evaluated as

$$\hat{\Pi}(-Q^2) = \frac{Q^2}{12\pi^2}\int_0^\infty ds \frac{R(s)}{s(s+Q^2)} . \tag{7}$$

The muon g-2 is the integration of HVP with a known kernel:

$$a_\mu^{\text{LO-HVP}} = \int dQ^2 K_{a_\mu}(m_\mu, Q^2)\hat{\Pi}(-Q^2) = 693.1(4.0)\cdot 10^{-10} , \tag{8}$$

which was the world consensus reported in the white-paper [Phys. Rept. 2020]. The result may be compared with the counterpert extracted by using FNAL/BNL measurements

$$a_\mu^{\text{LO-HVP}}|_{NoNewPhys} = a_\mu^{\text{FNAL/BNL}} - (a_\mu^{\text{QED}} + a_\mu^{\text{EW}} + a_\mu^{\text{(N)NLO-HVP}} + a_\mu^{\text{HLbL}}) \tag{9}$$
$$= 718.0(2.8)\cdot 10^{-10} .$$

The difference implies 5.1 σ tension. However, it is premature to regard the tension as a discovery of a BSM signal due to more than one reason: (1) CMD3 updates (next page), (2) Lattice QCD (next section).

Comparison of $a_\mu^{\pi\pi}$

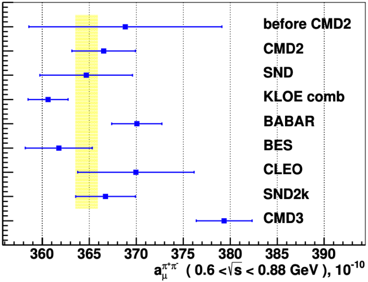

Figure 36: The $\pi^+\pi^-(\gamma)$ contribution to $a_\mu^{had,LO}$ from energy range $0.6 < \sqrt{s} < 0.88$ GeV obtained from this and other experiments.

Experiment	$a_\mu^{\pi^+\pi^-,LO}$, 10^{-10}
before CMD2	368.8 ± 10.3
CMD2	366.5 ± 3.4
SND	364.7 ± 4.9
KLOE	360.6 ± 2.1
BABAR	370.1 ± 2.7
BES	361.8 ± 3.6
CLEO	370.0 ± 6.2
SND2k	366.7 ± 3.2
CMD3	379.3 ± 3.0

Table 4: The $\pi^+\pi^-(\gamma)$ contribution to $a_\mu^{had,LO}$ from energy range $0.6 < \sqrt{s} < 0.88$ GeV obtained from this and other experiments.

- **Fig:** Comparison of $a_\mu^{\pi\pi}$. Quoted from CMD3-Collaboration papar (arXiv:2302.08834).
- Unknown systematics in data-driven approach? Systematic error dominance?

Table of Contents

Guide

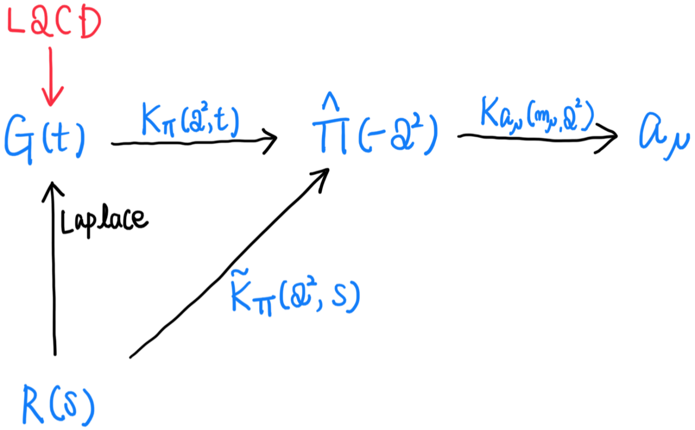

Lattice QCD measures the vector-current correlator $G_{\mu\nu}(t)$, whose scalar proportionality is denoted as $G(t)$. Their Fourier transformations give HVP.

Guide

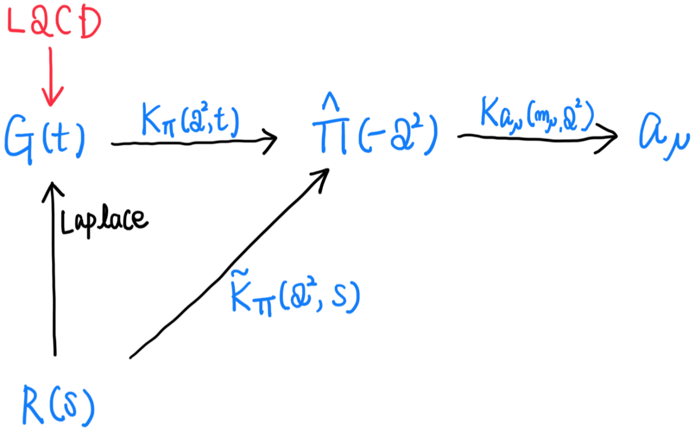

$$a_\mu = \sum_t W(m_\mu, t) G(t) \; , \quad W(m_\mu, t) = \int dQ^2 K_{a_\mu}(m_\mu, Q^2) K_\Pi(Q^2, t) \; . \quad (10)$$

Guide

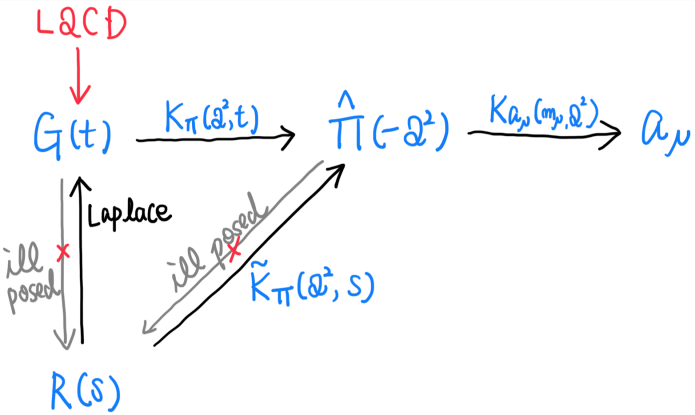
LQCD
G(t)
K_π(Q², t)
Π̂(−Q²)
K_{a_μ}(m_μ, Q²)
a_μ
Laplace
ill posed
ill posed
K̃_π(Q², s)
R(s)

Lattice Gauge Theory

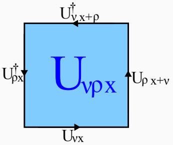

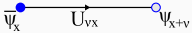

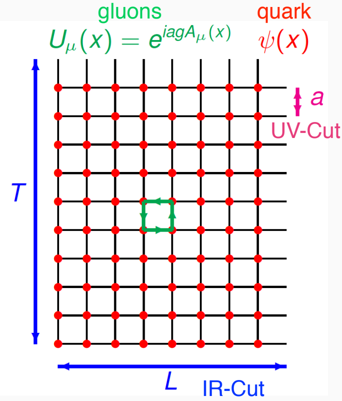

- Action: $S_{LQCD} = S_G[U, a] + S_F[\psi, \bar{\psi}, U, a]$.
- Gluon Field Strength ($U_{\nu x} \in SU(3)$):

$$S_G = \sum_{\nu\rho,x} \frac{2N_c}{g^2} \left[1 - \frac{\mathrm{tr}_c}{2N_c} \left[U_{\nu\rho,x} + U^\dagger_{\nu\rho,x} \right] \right]$$

$$\xrightarrow{a \to 0} \frac{1}{4} \int d^4x\; G_{\nu\rho,x} G_x^{\nu\rho}$$

- Quark Kinetic:

$$S_F = \sum_{xy} \bar{\psi}_x\, D[U, m, a]_{xy}\, \psi_y$$

$$\ni \bar{\psi}_x U_{\nu x} \psi_{x+\nu} \xrightarrow{a \to 0} \bar{\psi}_x (\partial_\nu + igA_{\nu x}) \psi_x \;.$$

Lattice QCD

Lattice QCD ($\ni a \to 0$): Non-Perturbative Def. of Continuum QCD.

- Similarly to perturbative-continum QCD, based on the quantum field theoretical constructions:
  ① Regularization (finite a) & ② Renormalization ($a \to 0$).
- No free parameter: Input quark masses are fixed to realize real-world hadron spectra.
- No approximation in path-integrals (Hybrid Monte Carlo (HMC) Algorithm).
- Various hadron spectra calculated by LQCD precisely explain experimental data.

Lattice QCD

- Continuum Extraporation:
  - A line of const. phys.: $a \to 0$ or equivalently $\beta(a) = 6/g^2(a) \to \infty$ is numerically taken with quark masses adjusted to keep hadron spectra ratio. Then, a plays a role of a renormalization scale μ.
  - Emergence of a mass gap $\Lambda \propto M_{had.}$ satisfying $a^{-1} \gg \Lambda \gg L^{-1}$ is implicitly assumed s.t. one can take a limit of $\Lambda a \to 0$ & $L\Lambda \to \infty$. Empirically, this is the case.
  - The above assumption (existence of the continuum limit) has not been mathematically verified. c.f. Clay's Millennium Prize Problems.

- Hybrid Monte Carlo Algorithm:
  - Molecular Dynamics (EoM) + Metropolis Test (Accept/Reject) for $U^i_{\nu x}$.
  - Generate gluon fields U^i with weight of $P[U^i] = \mathrm{Det} D[U^i]\ e^{-S_G[U^i]}/Z$.
  - Then $\langle O \rangle = \int_U\ P[U]O[U] = \sum_{i=1}^{N} O[U^i] + \mathcal{O}(1/\sqrt{N})$.

LQCD Meas. of HVP and $a_\mu^{\text{LO-HVP}}$

$\{U^{(i)}\}$: HMC

$\downarrow$

$D_f[U] \equiv D[U, m_f]$: Dirac Op.

$\downarrow$ Solve Dirac Eq.

$D_f^{-1}[U]$: Quark Propagator.

$\downarrow$

Vector Current Correlator

$$G^f_{\mu\nu}(x) = \langle (\bar\psi\gamma_\mu\psi)_x \, (\bar\psi\gamma_\nu\psi)_{y=0} \rangle \xrightarrow[\text{wick}]{}$$

$$C^f_{\mu\nu}(x) = -\left\langle \mathrm{ReTr}\left[\gamma_\mu \, D^{-1}_{f,x0}[U] \, \gamma_\nu \, D^{-1}_{f,0x}[U]\right] \right\rangle ,$$

$$D^f_{\mu\nu}(x) = \left\langle \mathrm{Re}\left[\mathrm{Tr}\left[\gamma_\mu \, D^{-1}_{f,xx}[U]\right] \mathrm{Tr}\left[\gamma_\nu \, D^{-1}_{f,yy}[U]\right]_{y=0}\right] \right\rangle ,$$

$\downarrow$

HVP: $\Pi^f_{\mu\nu}(Q) = \mathcal{F}.\mathcal{T}.[G^f_{\mu\nu}(x)]$,

g-2: $a^{\text{LO-HVP}}_{\mu,f} = (\frac{\alpha}{\pi})^2 \sum_t W(t, m_\mu^2) G^f(t)$.

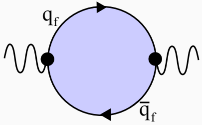

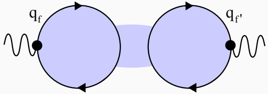

LQCD Meas. of HVP and $a_\mu^{\text{LO-HVP}}$

$\{U^{(i)}\}$: HMC

$\downarrow$

$D_f[U] \equiv D[U, m_f]$: Dirac Op.

$\downarrow$ Solve Dirac Eq.

$D_f^{-1}[U]$: Quark Propagator.

$\downarrow$

Vector Current Correlator

$$G^f_{\mu\nu}(x) = \langle (\bar\psi\gamma_\mu\psi)_x \, (\bar\psi\gamma_\nu\psi)_{y=0} \rangle \xrightarrow[\text{wick}]{}$$

$$C^f_{\mu\nu}(x) = -\left\langle \mathrm{ReTr}\left[\gamma_\mu \, D^{-1}_{f,x0}[U] \, \gamma_\nu \, D^{-1}_{f,0x}[U]\right] \right\rangle ,$$

$$D^f_{\mu\nu}(x) = \left\langle \mathrm{Re}\left[\mathrm{Tr}\left[\gamma_\mu \, D^{-1}_{f,xx}[U]\right] \, \mathrm{Tr}\left[\gamma_\nu \, D^{-1}_{f,yy}[U]\right]_{y=0}\right] \right\rangle ,$$

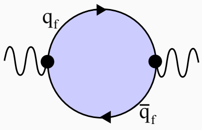

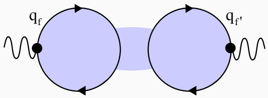

$\downarrow$

HVP: $\Pi^f_{\mu\nu}(Q) = \mathcal{F.T.}[G^f_{\mu\nu}(x)]$,

g-2: $a_{\mu,f}^{\text{LO-HVP}} = (\frac{\alpha}{\pi})^2 \sum_t W(t, m_\mu^2) G^f(t)$.

LQCD Meas. of HVP and $a_\mu^{\text{LO-HVP}}$

$\{U^{(i)}\}$: HMC

$\downarrow$

$D_f[U] \equiv D[U, m_f]$: Dirac Op.

$\downarrow$ Solve Dirac Eq.

$D_f^{-1}[U]$: Quark Propagator.

$\downarrow$

Vector Current Correlator

$$G^f_{\mu\nu}(x) = \langle (\bar\psi\gamma_\mu\psi)_x \, (\bar\psi\gamma_\nu\psi)_{y=0} \rangle \xrightarrow[\text{wick}]{}$$

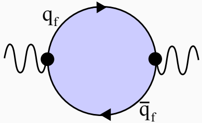

$$C^f_{\mu\nu}(x) = -\left\langle \mathrm{ReTr}\left[\gamma_\mu \, D^{-1}_{f,x0}[U] \; \gamma_\nu \, D^{-1}_{f,0x}[U]\right] \right\rangle ,$$

$$D^f_{\mu\nu}(x) = \left\langle \mathrm{Re}\left[\mathrm{Tr}\left[\gamma_\mu \, D^{-1}_{f,xx}[U]\right] \; \mathrm{Tr}\left[\gamma_\nu \, D^{-1}_{f,yy}[U]\right]_{y=0}\right] \right\rangle ,$$

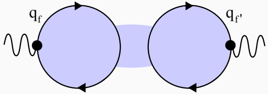

$\downarrow$

HVP: $\Pi^f_{\mu\nu}(Q) = \mathcal{F}.\mathcal{T}.[G^f_{\mu\nu}(x)]$,

g-2: $a^{\text{LO-HVP}}_{\mu,\,f} = (\frac{\alpha}{\pi})^2 \sum_t W(t, m_\mu^2) G^f(t)$.

Table of Contents

Budapest-Marseille-Wuppertal Collaboration

Sz. Borsanyi, Z. Fodor, J.N. Guenther, C. Hoelbling, S.D. Katz, L. Lellouch, T. Lippert, K. Miura, L. Parato, K.K. Szabo, F. Stokes, B.C. Toth, Cs. Torok, and L. Varnhorst.

References

- arXiv:2002.12347. Published in Nature 2021.
- Phys. Rev. Lett. **121**, no. 2, 022002 (2018).
- Phys. Rev. D **96**, no. 7, 074507 (2017).

BMW Simulation Setup

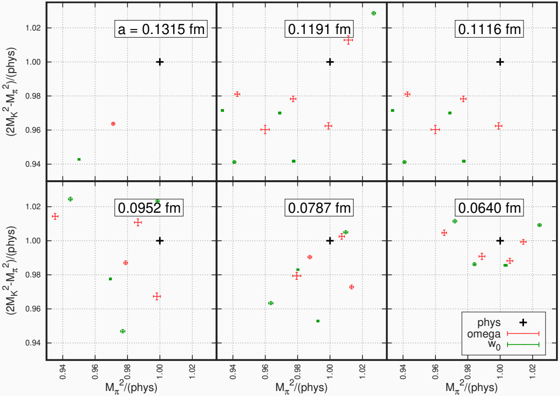

- 6 lattice spacings, 28 simulations around phys. pt.
- $N_f = (2+1+1)$ staggered quarks. ($m_u = m_d$)
- Large Volume: $(L, T) \sim (6, 9-12)fm$. c.f. Helium nucleous diameter is $3.8fm$.
- Scale Setting (0.4%): $M_\Omega^{lat} = \frac{M_{\Omega^-}^{phys} a[fm]}{\hbar c}$.

Input Quark Mass (m_{ud}^0, m_s, m_c) Tuning

$$\left[\frac{M_\pi^2}{M_\Omega^2}\right]_{lat} \simeq \left[\frac{M_{\pi^0}^2}{M_{\Omega^-}^2}\right]_{phys}, \quad \left[\frac{M_K^2 - M_\pi^2/2}{M_\Omega^2}\right]_{lat} \simeq \left[\frac{(M_{K^+}^2 + M_{K^0}^2 - M_{\pi^0}^2)/2}{M_{\Omega^-}^2}\right]_{phys}, \quad \frac{m_c}{m_s} = 11.85 \,.$$

Integrand $W(t, m_\mu^2)C^{ud}(t)$

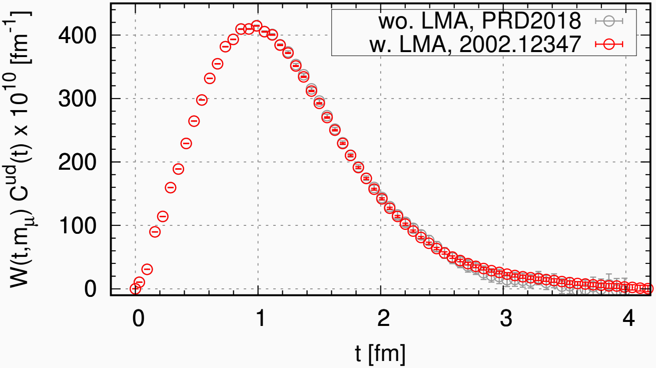

Fig: The integrand of $a_{\mu,\,ud}^{\text{LO-HVP}} = \sum_t W(t, m_\mu^2)C^{ud}(t)$. BMW-2020/2018 data with the finest lattice $a = 0.064\ fm$.

Long Distance Control

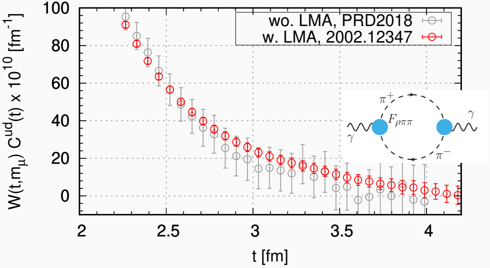

Fig: Long-distance region of the integrand $W(t, m_\mu^2)C^{ud}(t)$. BMW-2020/2018, $a = 0.064\ fm$.

- Needs long distanc control: $\hbar c/M_\pi \sim 4\ fm$. The kernel $W(t, m_\mu^2)$ makes a long tail.
- Low Mode Averaging (LMA) greatly reduces the long distance errors.
- LMA [Neff et al. PRD2001, Giusti et al. JHEP2004]: Lanczos-like method to extract exactly (not stochastically) low eigen values/vectors of Dirac operator $D[U]$.
- $\mathcal{O}(1000)$ eigen values/vectors $\lesssim m_s/2$ have been determined.

COntinuum Extrapolation of $a_{\mu,\,ud}^{\text{LO-HVP}}$

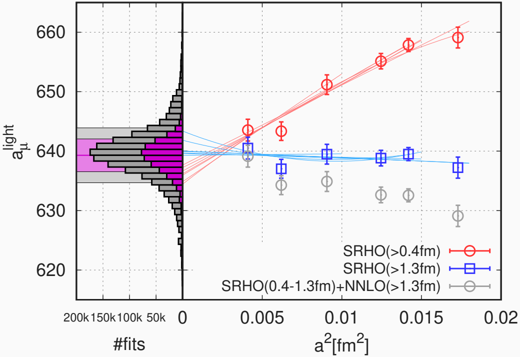

- **Fig:** Continuum extrapolation of $a_{\mu,\,ud}^{\text{LO-HVP}}$. From [BMW Nature 593 (2021) 7857].
- SRHO denotes staggered-ρ-π-γ model, which corrects known lattice spacing artefact steming from the taste-symmetry breaking, in advance to the continuum extrapolations.

$$a_{\mu,\,ud}^{\text{LO-HVP}} = 639.3(2.0)(4.2)\ , \quad 0.7\%\ \text{Prec.} \tag{11}$$

c.f. White Paper: 1.8% Prec.

QED and Strong-Isospin Breaking Corrections

$$\mathcal{O}(\alpha) \sim \mathcal{O}\left(\frac{m_d - m_u}{\Lambda_{QCD}}\right) \sim 1\%\ \text{Correction} \quad .$$

Isospin Breaking Perturbatively

- Iso-symm. LQCD (U) + Stochastic QED (A_μ with $P \propto e^{-S_\gamma}$).

$$Z = \int \mathcal{D}U\, e^{-S_g[U]} \int \mathcal{D}A\, e^{-S_\gamma[A]} \prod_{f=u,d,s,c} \mathrm{Det}\, D[Ue^{ieq_f A}, m_f]\,. \tag{12}$$

- QED_L [Hayakawa PTP2008] in Coulomb gauge. c.f. Gauss's Law.

- Expand w.r.t. $\alpha = e^2/(4\pi)$ and $\delta m = m_d - m_u$:

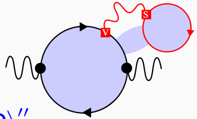

$$\langle O[Ue^{ie_v q_f A}, m_f]\rangle = \langle O[U, m_f^0]\rangle_U$$
$$+(\delta m/m_{ud}^0)\langle O\rangle'_m + e_v^2\langle O\rangle''_{vv} + e_v e_s \langle O\rangle''_{vs} + e_s^2\langle O\rangle''_{ss}\,,$$

e.g.

$$\langle O\rangle''_{vs} = \left\langle \left\langle \frac{\partial O}{\partial e_v}\Big|_{e_v\to 0} \times \frac{\partial}{\partial e_s} \prod_f \frac{\mathrm{Det}\, D[Ue^{ie_s q_f A}, m_f^0]}{\mathrm{Det}\, D[U, m_f^0]} \right\rangle_A \Big|_{e_s\to 0} \right\rangle_U . \tag{13}$$

$\partial O/\partial e \simeq (O_{+e} - O_{-e})/e\,.$

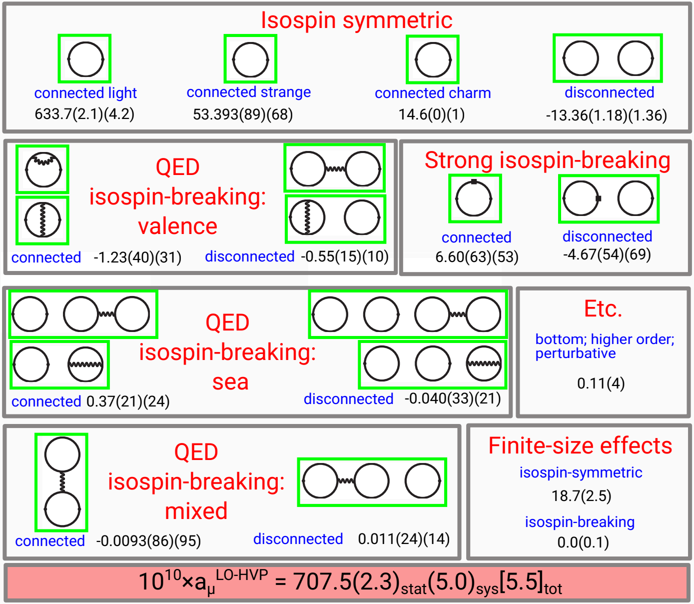

Fig: Quoted from Nature **593** (2021) no.7857.

BMW $a_\mu^{\text{LO-HVP}}$ Summary and Comparison

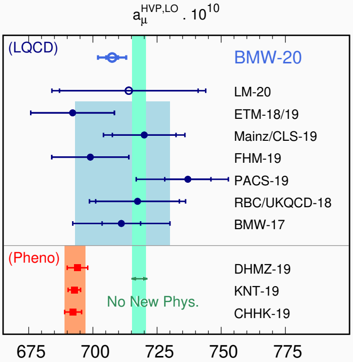

Figure: LO-HVP ($O(\alpha_0^2)$) muon g-2 comparison.

(No New Phys.)
= (FNAL/BNL) − (SM wo. LO-HVP).

BMW2020(Nature 593 (2021) 7857)

- $\mathbf{a}_{\mu,\mathbf{BMW}}^{\text{LO-HVP}} = \mathbf{707.5(2.3)(5.0)\cdot 10^{-10}}$, **0.8%**

  c.f. $a_{\mu,WP}^{\text{LO-HVP}} = 711.6(18.4)\cdot 10^{-10}$ (blue-band).

- $\mathbf{a}_{\mu,\mathbf{BMW}}^{\text{LO-HVP}}$ vs. *No New Physics*: 1.7σ tension.

  c.f. Pheno (red-band) vs. No New Physics: 5.1σ tension, where CMD3 is not yet included.

- $\mathbf{a}_{\mu,\mathbf{BMW}}^{\text{LO-HVP}}$ vs. Pheno (red-band):

  2.1σ tension.

Table of Contents

Guide

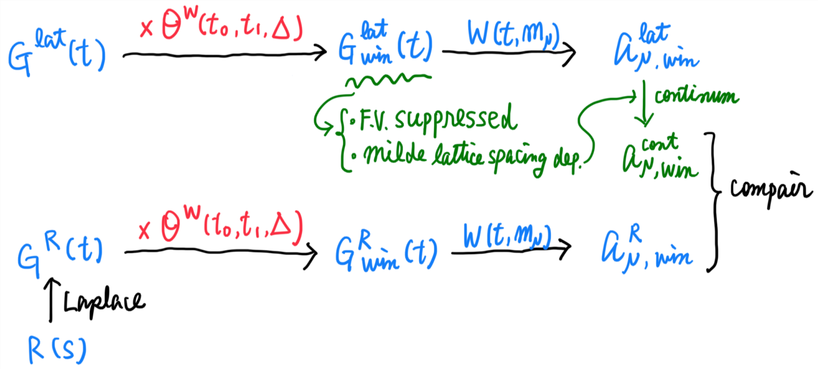

$$\Theta^W(t,t_0,t_1,\Delta) = \frac{1}{2}\left(\tanh\left[\frac{t-t_0}{\Delta}\right] - \tanh\left[\frac{t-t_1}{\Delta}\right]\right)\,. \qquad (14)$$

Integrand of $a_{\mu,ud}^{\text{LO-HVP}}$ I

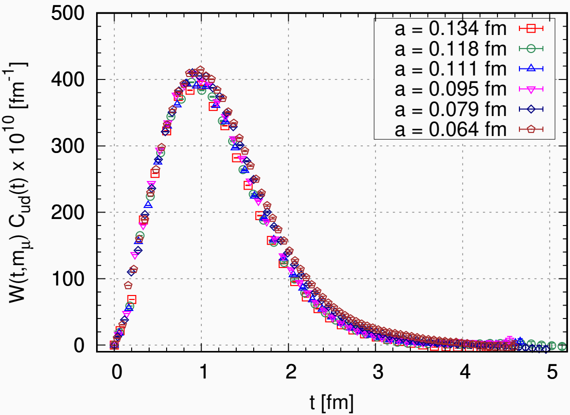

$$a_{\mu}^{\text{LO-HVP}} = \sum_{t} W(t, m_{\mu}) C^{lat}(t) \,, \quad (15)$$

$$c.f.\ C^{pheno}(t) = \int_{0}^{\infty} ds \sqrt{s} R_{had}(s) e^{-\sqrt{s}|t|} \,. \quad (16)$$

Integrand of $a_{\mu,ud}^{\text{LO-HVP}}$ II

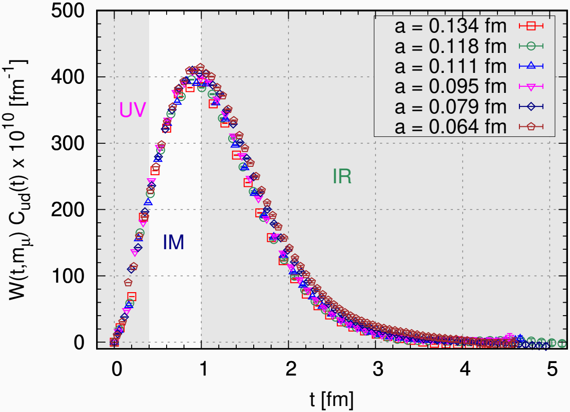

$$a_\mu^{\text{LO-HVP}} = \sum_t W(t, m_\mu) C^{lat}(t) \,, \tag{17}$$

$$c.f.\ C^{pheno}(t) = \int_0^\infty ds\sqrt{s} R_{had}(s) e^{-\sqrt{s}|t|} \,. \tag{18}$$

Window Method

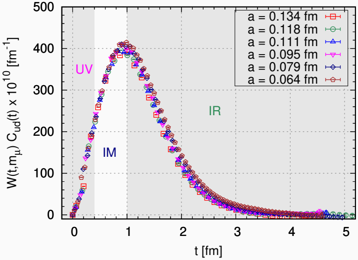

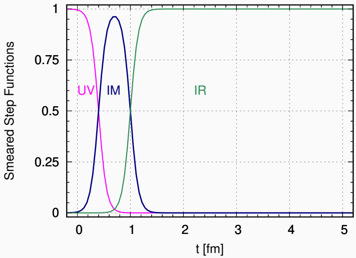

$$\text{UV: } S_{UV}(t) = 1.0 - (1.0 + \tanh[(t - t_0)/\Delta])/2\,, \tag{19}$$

$$\text{IM: } S_{IM}(t) = \frac{1}{2}\left(\tanh\left[\frac{t-t_0}{\Delta}\right] - \tanh\left[\frac{t-t_1}{\Delta}\right]\right) =: \Theta^W(t, t_0, t_1, \Delta)\,, \tag{20}$$

$$\text{IR: } S_{IR}(t) = (1.0 + \tanh[(t - t_1)/\Delta])/2\,, \tag{21}$$

$$\text{We shall adopt } t_0 = 0.4fm\,, \quad t_1 = 1.0fm\,, \quad \Delta = 0.15fm\,. \tag{22}$$

c.f. RBC-UKQCD, arXiv: 1801.07224

Window IR Threshold I

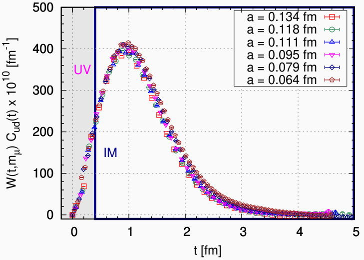

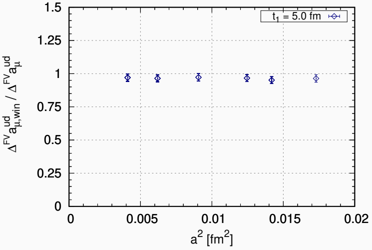

- FV: Spatially n-th wrapping pions w. pion form factor. [M. Hansen & A. Pattella, PRL2019, arXiv:200403935.]
- $t_0 = 0.4 fm$ (fixed) , $t_1 = 5.0 fm$.

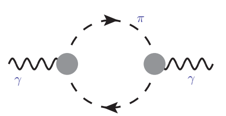

Window IR Threshold II

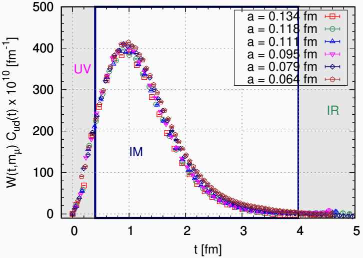

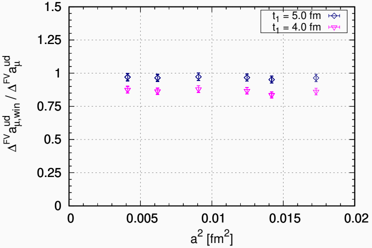

- FV: Spatially *n*-th wrapping pions w. pion form factor.
  [M. Hansen & A. Pattella, PRL2019, arXiv:200403935.]
- $t_0 = 0.4 fm$ (fixed) , $\quad t_1 = 4.0 fm$.

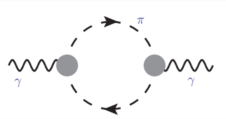

Window IR Threshold III

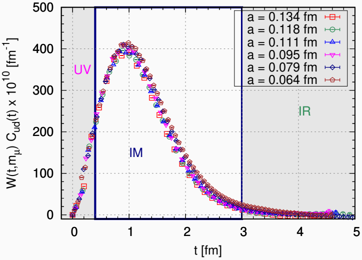

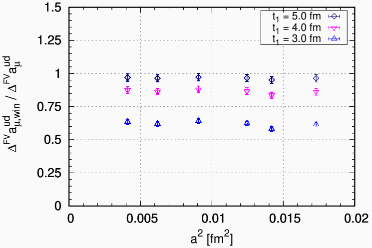

- FV: Spatially n-th wrapping pions w. pion form factor.
  [M. Hansen & A. Pattella, PRL2019, arXiv:200403935.]
- $t_0 = 0.4fm$ (fixed) , $t_1 = 3.0fm$.

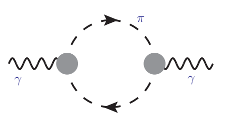

Window IR Threshold IV

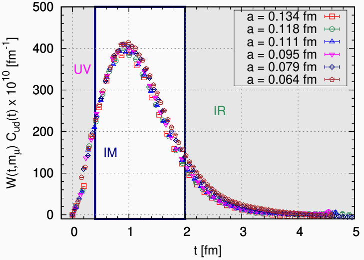

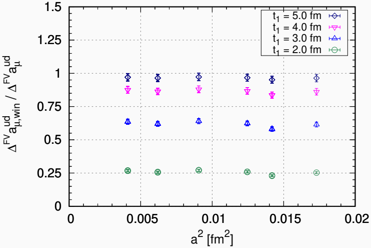

- FV: Spatially n-th wrapping pions w. pion form factor.
  [M. Hansen & A. Pattella, PRL2019, arXiv:200403935.]
- $t_0 = 0.4 fm$ (fixed) , $t_1 = 2.0 fm$.

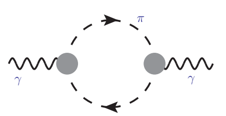

Window IR Threshold V

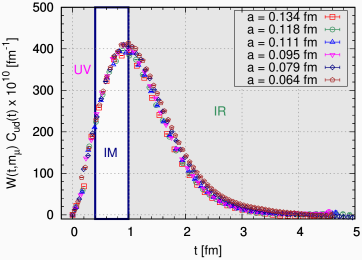

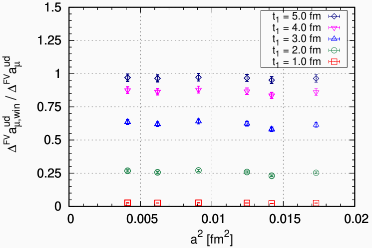

- FV: Spatially *n*-th wrapping pions w. pion form factor. [M. Hansen & A. Pattella, PRL2019, arXiv:200403935.]
- $t_0 = 0.4 fm$ (fixed) , $t_1 = 1.0 fm$.

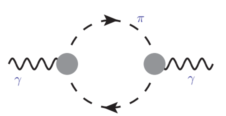

Window UV Threshold I

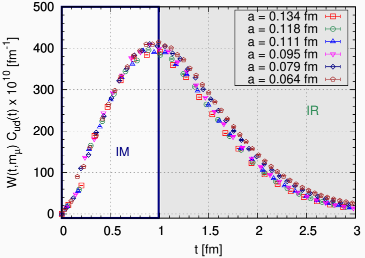

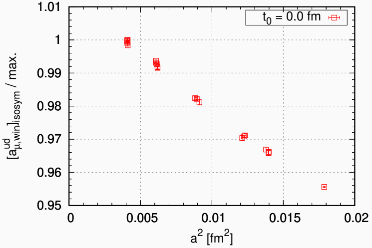

$t_0 = 0.0 fm$, $t_1 = 1.0 fm =$ fixed .

Window UV Threshold II

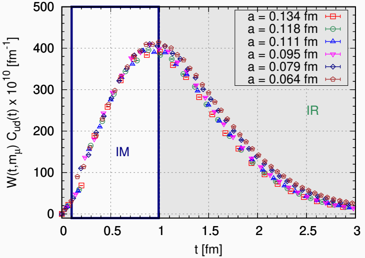

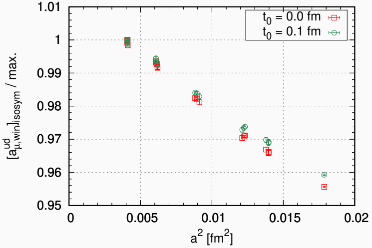

$$t_0 = 0.1\,fm\,, \qquad t_1 = 1.0\,fm = \text{fixed}\,.$$

Window UV Threshold III

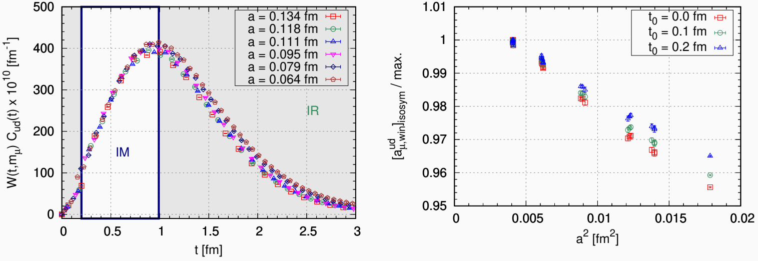

$$t_0 = 0.2 fm \,, \qquad t_1 = 1.0 fm = \text{fixed} \,.$$

Window UV Threshold IV

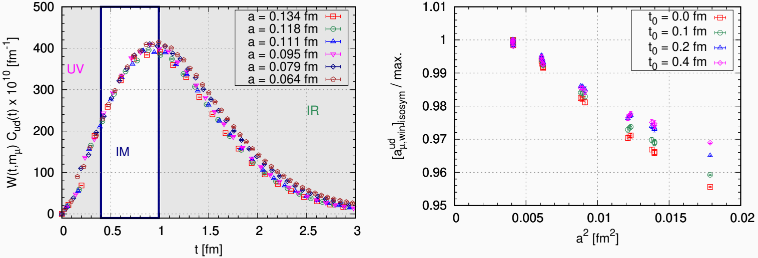

$$t_0 = 0.4 fm \,, \qquad t_1 = 1.0 fm = \text{fixed} \,.$$

Window Method Comparison

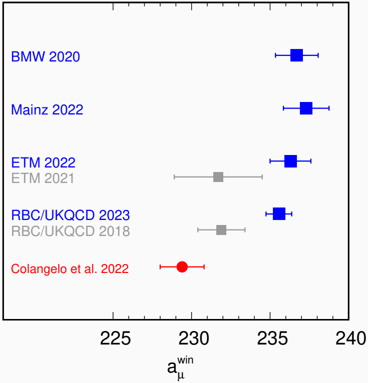

- The total contributions to the intermediate window a_μ^{win} from the latest LQCDs (■) becomes consistent.
- N.B.: For a ud-quark contributions, FHMc has also provided the latest window results [arXiv:2301.08274].
- The LQCD shows more than 3.5σ tension to the latest data-driven method (●).

Lattice Spacing Comparison

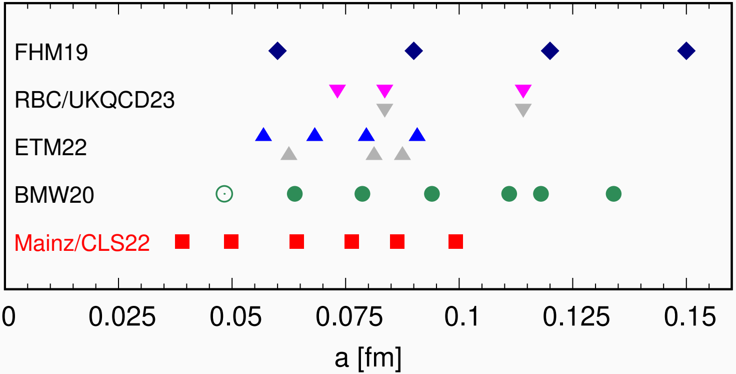

Table of Contents

Guide

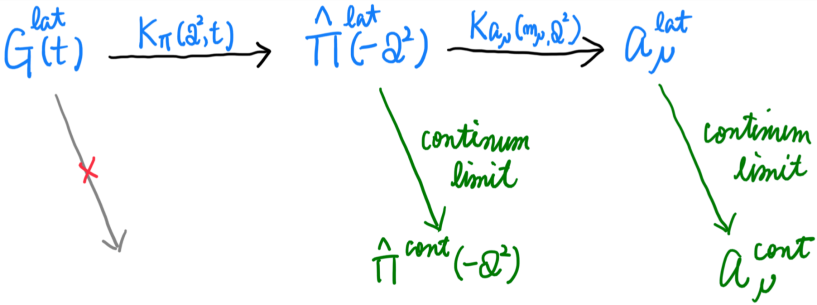
$G^{lat}(t)$
$K_\pi(Q^2, t)$
$\hat{\Pi}^{lat}(-Q^2)$
$K_{a_\mu}(m_\mu, Q^2)$
a_μ^{lat}
continuum limit
continuum limit
$\hat{\Pi}^{cont}(-Q^2)$
a_μ^{cont}

Guide

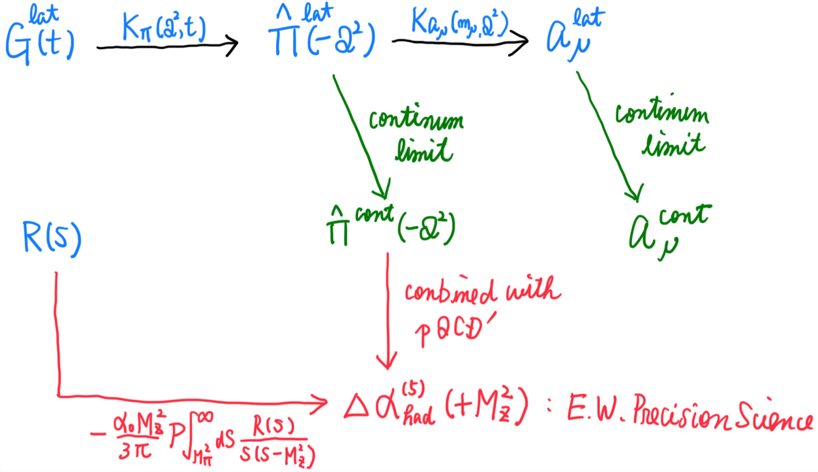

$G^{lat}(t)$
$K_\pi(Q^2,t)$
$\hat{\Pi}^{lat}(-Q^2)$
$K_{a_\mu}(m_\mu, Q^2)$
a_μ^{lat}
continuum limit
continuum limit
$R(s)$
$\hat{\Pi}^{cont}(-Q^2)$
a_μ^{cont}
combined with pQCD
$-\frac{\alpha_0 M_Z^2}{3\pi} P\int_{M_\pi^2}^{\infty} ds \frac{R(s)}{s(s-M_Z^2)}$
$\Delta\alpha_{had}^{(5)}(+M_Z^2)$: E.W. Precision Science

Five-Flavor QED Running Coupling $\Delta\alpha^{(5)}_{\rm had}(s)$

- QED Running Coupling:

$$\alpha_{QED}(s) = \frac{\alpha_0}{1 - \Delta\alpha_{lep}(s) - \Delta\alpha_{had}(s)} \ , \tag{23}$$

where $\alpha_0 = 1/137.03\cdots$ and $\Delta\alpha_{had}(s) = 4\pi\alpha_0\hat{\Pi}(s)$.

- LQCD Target:

$$\Delta\alpha^{(5)}_{\rm had}(-Q^2) = 4\pi\alpha_0\hat{\Pi}^{udscb}(-Q^2) \ , \quad Q^2 \sim \mathcal{O}(1)GeV^2 \text{ spacelike} \ . \tag{24}$$

- [Crivellin et al. PRL2020]: If $a_\mu^{\text{LO-HVP}}$ gets closer to NoNewPhys, the tension increases at EW-Global fit. c.f. [M.Passera et al. PRD08].

- [BMW-2020, 2002.12347]: The tension is not necessarily suggested by looking at LQCD data $\Delta\alpha_{\rm had}(-10GeV^2)$–$\Delta\alpha_{\rm had}(-1GeV^2)$.

- [Mainz/CLS-2022]: Based on LQCD $\Delta\alpha_{\rm had}(-Q^2)$ + pQCD$'$, investigated one of the EW-parameters: $\Delta\alpha^{(5)}_{\rm had}(+M_Z^2)$, Z-pole (timelike) .

Mainz HVP Working Group

M. Cè, A. Géradin, G. Hippel, R. Hudspith, S. Kuberski, H.B. Meyer, K. Miura, D. Mohler, K. Ottnad, S. Paul, A. Risch, T. San José, J. Wilhelm, and H. Wittig.

JHEP2022 and arXiv:2206.06582 [hep-lat]

Mainz/CLS Ensembles

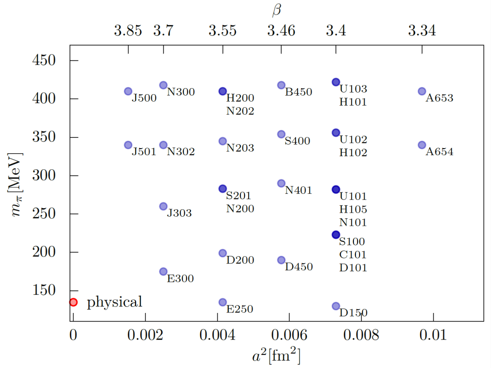

CLS Ensembles: [Bruno et al. JHEP2015].

- $\mathcal{O}(a)$ Imp. Wilson-Clover Fermions [Gérardin et.al. '18, ALPHAc '20, Fritzsch '18].
- $N_f = (2{+}1)$ (w. valence charms, wo. loops).
- $\mathcal{O}(a^2)$ Improved Lüscher-Weisz Gauge Action.
- $M_\pi L = 4.1 - 6.4$.
- Open/Periodic Boundary Conditions.
- Scale setting: $\sqrt{8t_0^{phys}} = 0.415(4)(2)\ fm$ [Bruno et.al. PRD2017].
- Low-Mode Deflation, Hierarchical Probe, Frequency-Splitting.

$\Delta\alpha^{(5)}_{\rm had}(-Q^2)$ Summary

Error Type	%	Comments
statistical	1.1	simulation based
chiral/continuum extrap.	0.1	simulation based
scale setting	0.7	simulation based
isospion breaking	0.3	simulation based
charm sea-quark	0.3	D-meson pheno.
charm disconnected	~ 0.01	1% of uds-disc. c.f. [BMW-PRL18]
bottom	0.3	w. time-moments by [HPQCD-PRD2015]

Table: Error Budget in $\Delta\alpha^{(5)}_{\rm had}(-5GeV^2) = 0.00716(8)_{sta}(0)_{fit}(5)_{scale}(2)_{isb}(2)_{c\text{-}sea}(2)_{b}[9]$.

- $\Delta\alpha^{(5)}_{\rm had}(-Q_0^2)|_{\rm central} = \Delta\alpha^{\rm Mainz}_{\rm had}(-Q_0^2)|_{\rm central}$ from $N_f = 2+1$ ensembles.
- Isospin breaking, charm-sea/disc, and bottom effects are considered into systematic errors.

Comparison of $\Delta\alpha^{(5)}_{\rm had}(-Q^2)$

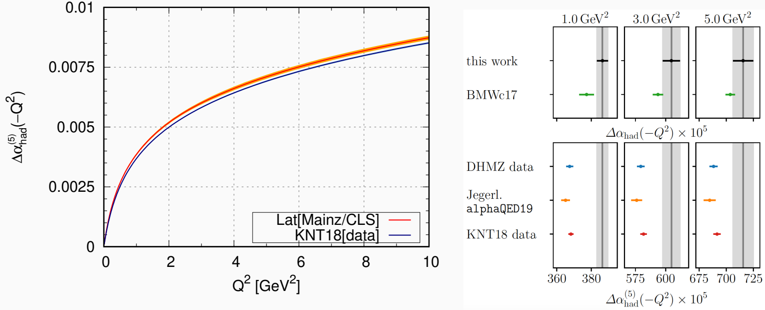

- **Fig.** Left: LQCD [Mainz-JHEP22] vs. Pheno(KNT18[data], [KNT-PRD18]) for $\Delta\alpha^{(5)}_{\rm had}(-Q^2) \propto \hat{\Pi}^{u,d,s,c,b}(-Q^2)$. Right: Detailed comparisons.
- Mainz results are consistent with BMWc17 but larger than phenomenological estimates with a few sigma tension.
- Larger $\Delta\alpha^{(5)}_{\rm had}(-Q^2) \Longleftrightarrow$ larger $a_\mu^{\text{LO-HVP}}$.

Euclidean Split Method

- Euclidean Split Method [Jegerlehner'08]:

$$\Delta\alpha^{(5)}_{\text{had}}(M_Z^2) = \Delta\alpha^{(5)}_{\text{had}}(-Q_0^2) \longleftarrow \text{LQCD}$$

$$+\left[\Delta\alpha^{(5)}_{\text{had}}(-M_Z^2) - \Delta\alpha^{(5)}_{\text{had}}(-Q_0^2)\right] \longleftarrow \text{pQCD}'$$

$$+\left[\Delta\alpha^{(5)}_{\text{had}}(M_Z^2) - \Delta\alpha^{(5)}_{\text{had}}(-M_Z^2)\right] \longleftarrow 0.000045(\text{pQCD}) \,.$$

- c.f. Usual R-ratio Method (Data-Driven Pheno.):

$$\Delta\alpha^{(5)}_{\text{had}}(M_Z^2) = -\frac{\alpha_0 M_Z^2}{3\pi}\,\mathcal{P}\int_{4M_\pi^2}^{\infty} ds\,\frac{R(s)}{s(s-M_Z^2)}\,.$$

pQCD′[Adler]

- Naive expression for higher energy corrections:

$$\left[\Delta\alpha^{(5)}_{\rm had}(-M_Z^2) - \Delta\alpha^{(5)}_{\rm had}(-Q_0^2)\right] = \frac{\alpha_0}{3\pi}(M_Z^2 - Q_0^2)\int_{m^2_{\pi^0}}^{\infty} ds \frac{R(s)}{(s+Q_0^2)(s+M_Z^2)} \,.$$

- Higher energy corrections w.r.t. Adler function $D(-Q^2)$:

$$\left[\Delta\alpha^{(5)}_{\rm had}(-M_Z^2) - \Delta\alpha^{(5)}_{\rm had}(-Q_0^2)\right] = \frac{\alpha_0}{3\pi}\int_{Q_0^2}^{M_Z^2} \frac{dQ^2}{Q^2} D(-Q^2)\,, \qquad (25)$$

where $D(-Q^2) = (3\pi/\alpha_0)[s\, d\Delta\alpha^{(5)}_{\rm had}(s)/ds]_{s=-Q^2}$.

- For the Adler function, pQCD relatively works:
  pQCD′[Adler] = pQCD + Operator Product Expn. + Padè fits
  captures J/Ψ and Υ resonances.

pQCD′[Adler]

- Naive expression for higher energy corrections:

$$\left[\Delta\alpha^{(5)}_{\rm had}(-M_Z^2) - \Delta\alpha^{(5)}_{\rm had}(-Q_0^2)\right] = \frac{\alpha_0}{3\pi}(M_Z^2 - Q_0^2)\int_{m^2_{\pi^0}}^{\infty} ds \frac{R(s)}{(s+Q_0^2)(s+M_Z^2)} \; .$$

- Higher energy corrections w.r.t. Adler function $D(-Q^2)$:

$$\left[\Delta\alpha^{(5)}_{\rm had}(-M_Z^2) - \Delta\alpha^{(5)}_{\rm had}(-Q_0^2)\right] = \frac{\alpha_0}{3\pi}\int_{Q_0^2}^{M_Z^2} \frac{dQ^2}{Q^2} D(-Q^2) \; , \qquad (25)$$

where $D(-Q^2) = (3\pi/\alpha_0)[s\, d\Delta\alpha^{(5)}_{\rm had}(s)/ds]_{s=-Q^2}$.

- For the Adler function, pQCD relatively works:

  pQCD′[Adler] = pQCD + Operator Product Expn. + Padè fits

  captures J/Ψ and Υ resonances.

Adler Function

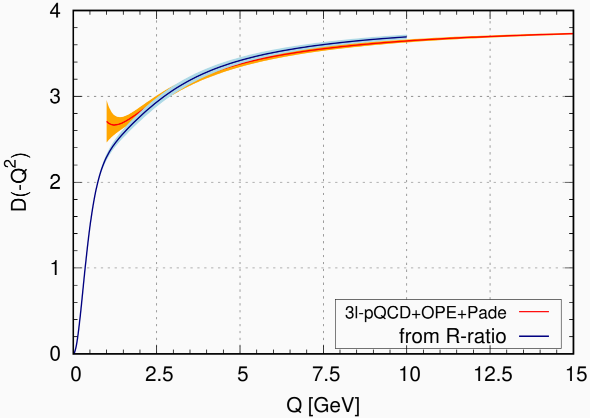

Red: $D(-Q^2)$ using pQCD′ = 3l-pQCD + OPE + Padè.

Blue: $D(-Q^2) = Q^2 \int_{4M_\pi^2}^{\infty} ds\, R(s)/(s+Q^2)^2$.

QED Coupling at Z-pole with Mainz LQCD

$$\Delta\alpha^{(5)}_{\rm had}(M_Z^2) = \underbrace{\Delta\alpha^{(5)}_{\rm had}(-5GeV^2)}_{\text{LQCD: } 0.00716(9)} + \underbrace{\left[\Delta\alpha^{(5)}_{\rm had}(-M_Z^2) - \Delta\alpha^{(5)}_{\rm had}(-5GeV^2)\right]}_{\text{pQCD}'\text{[Adler]: } 0.02053(12)} + \underbrace{\left[\Delta\alpha^{(5)}_{\rm had}(M_Z^2) - \Delta\alpha^{(5)}_{\rm had}(-M_Z^2)\right]}_{\text{pQCD: } 4.5(0.2)\cdot 10^{-6}}$$

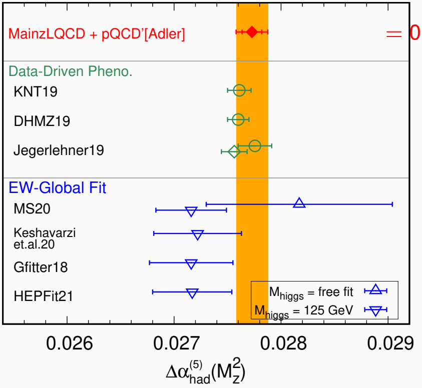

$$= 0.02773(9)_{\rm lat}(2)_{\text{c-sea/b}}(12)_{\rm pQCD'}\,[15(0.5\%)]_{\rm tot}\,.$$

$$\Delta\alpha^{(5)}_{\rm had}(M_Z^2) = -\frac{\alpha_0 M_Z^2}{3\pi}\,\mathcal{P}\int_{4M_\pi^2}^{\infty} ds\,\frac{R(s)}{s(s-M_Z^2)}$$

$\Delta\alpha^{(5)}_{\rm had}(M_Z^2)$ as a fit parameter in EW-Global fits.

Figure: 5-flavor quark/hadron contributions to QED coupling at Z-pole.

QED Coupling at Z-pole with Mainz LQCD

$$\Delta\alpha^{(5)}_{\rm had}(M_Z^2) = \underbrace{\Delta\alpha^{(5)}_{\rm had}(-5GeV^2)}_{\text{LQCD: }0.00716(9)} + \underbrace{\left[\Delta\alpha^{(5)}_{\rm had}(-M_Z^2) - \Delta\alpha^{(5)}_{\rm had}(-5GeV^2)\right]}_{\text{pQCD}'\text{[Adler]: }0.02053(12)} + \underbrace{\left[\Delta\alpha^{(5)}_{\rm had}(M_Z^2) - \Delta\alpha^{(5)}_{\rm had}(-M_Z^2)\right]}_{\text{pQCD: }4.5(0.2)\cdot 10^{-6}}$$

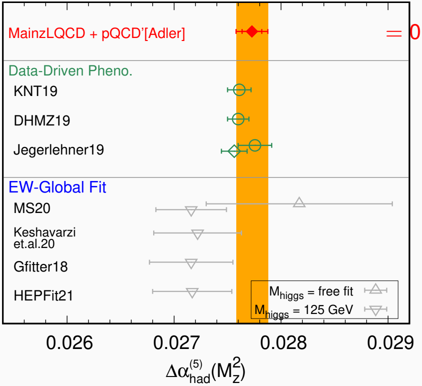

$$= 0.02773(9)_{\rm lat}(2)_{\text{c-sea/b}}(12)_{\rm pQCD'}\,[15(0.5\%)]_{\rm tot}\,.$$

$$\Delta\alpha^{(5)}_{\rm had}(M_Z^2) = -\frac{\alpha_0 M_Z^2}{3\pi}\,\mathcal{P}\int_{4M_\pi^2}^{\infty} ds\,\frac{R(s)}{s(s-M_Z^2)}$$

- Our result ♦ is consistent with all results using R-ratio.
- Recall 2.2σ tension in $\Delta\alpha^{(5)}_{\rm had}(-5GeV^2)$. The tension has diminished due to the error from higher energy.

Figure: 5-flavor quark/hadron contributions to QED coupling at Z-pole.

QED Coupling at Z-pole with Mainz LQCD

$$\Delta\alpha^{(5)}_{\rm had}(M_Z^2) = \underbrace{\Delta\alpha^{(5)}_{\rm had}(-5GeV^2)}_{\text{LQCD: } 0.00716(9)} + \underbrace{\left[\Delta\alpha^{(5)}_{\rm had}(-M_Z^2) - \Delta\alpha^{(5)}_{\rm had}(-5GeV^2)\right]}_{\text{pQCD}'\text{[Adler]: } 0.02053(12)} + \underbrace{\left[\Delta\alpha^{(5)}_{\rm had}(M_Z^2) - \Delta\alpha^{(5)}_{\rm had}(-M_Z^2)\right]}_{\text{pQCD: } 4.5(0.2)\cdot 10^{-6}}$$

$$= 0.02773(9)_{\rm lat}(2)_{\text{c-sea/b}}(12)_{\rm pQCD'}\,[15(0.5\%)]_{\rm tot}\ .$$

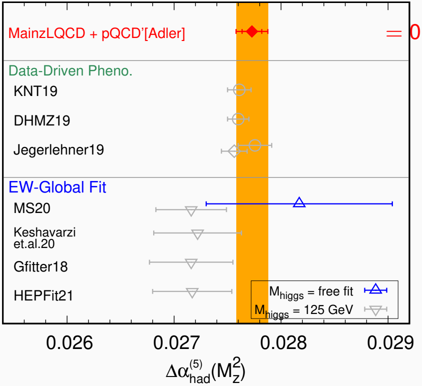

Figure: 5-flavor quark/hadron contributions to QED coupling at Z-pole.

$\Delta\alpha^{(5)}_{\rm had}(M_Z^2)$ as a fit parameter in EW-Global fits.

Our result ♦ is consistent with △, an output in EW-Global fits with M_{higgs} left as a fit parameter (no-prior).

QED Coupling at Z-pole with Mainz LQCD

$$\Delta\alpha^{(5)}_{had}(M_Z^2) = \underbrace{\Delta\alpha^{(5)}_{had}(-5GeV^2)}_{\text{LQCD: } 0.00716(9)} + \underbrace{\left[\Delta\alpha^{(5)}_{had}(-M_Z^2) - \Delta\alpha^{(5)}_{had}(-5GeV^2)\right]}_{\text{pQCD}'\text{[Adler]: } 0.02053(12)} + \underbrace{\left[\Delta\alpha^{(5)}_{had}(M_Z^2) - \Delta\alpha^{(5)}_{had}(-M_Z^2)\right]}_{\text{pQCD: } 4.5(0.2)\cdot 10^{-6}}$$

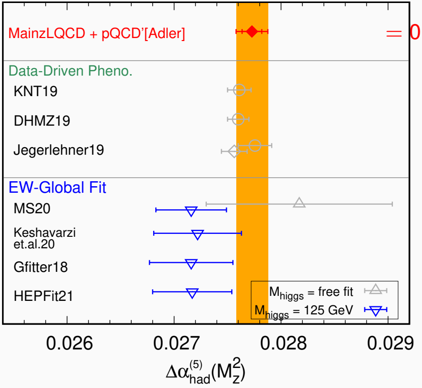

$$= 0.02773(9)_{\text{lat}}(2)_{\text{c-sea/b}}(12)_{\text{pQCD}'}\,[15(0.5\%)]_{\text{tot}}\,.$$

Figure: 5-flavor quark/hadron contributions to QED coupling at Z-pole.

$\Delta\alpha^{(5)}_{had}(M_Z^2)$ as a fit parameter in EW-Global fits.

If $M_{higgs} = 125\ GeV$ is used as a prior, EW-Global fits gives smaller $\Delta\alpha^{(5)}_{had}(M_Z^2)$ as indicated by $\triangledown$. But the tension is at most 1.3σ. c.f. [Crivellin et al, PRL2020].

LQCD does not necessarily show a clear tension to the SM.

QED Coupling at Z-pole with Mainz LQCD

$$\Delta\alpha^{(5)}_{\rm had}(M_Z^2) = \underbrace{\Delta\alpha^{(5)}_{\rm had}(-5GeV^2)}_{\text{LQCD: }0.00716(9)} + \underbrace{\left[\Delta\alpha^{(5)}_{\rm had}(-M_Z^2) - \Delta\alpha^{(5)}_{\rm had}(-5GeV^2)\right]}_{\text{pQCD}'\text{[Adler]: }0.02053(12)} + \underbrace{\left[\Delta\alpha^{(5)}_{\rm had}(M_Z^2) - \Delta\alpha^{(5)}_{\rm had}(-M_Z^2)\right]}_{\text{pQCD: }4.5(0.2)\cdot 10^{-6}}$$

$$= 0.02773(9)_{\rm lat}(2)_{\text{c-sea/b}}(12)_{\rm pQCD'}\,[15(0.5\%)]_{\rm tot}\,.$$

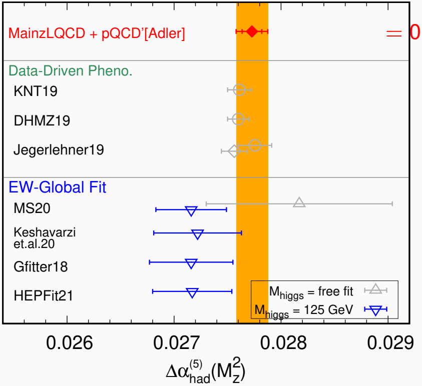

Figure: 5-flavor quark/hadron contributions to QED coupling at Z-pole.

$\Delta\alpha^{(5)}_{\rm had}(M_Z^2)$ as a fit parameter in EW-Global fits.

If $M_{higgs} = 125\ GeV$ is used as a prior, EW-Global fits gives smaller $\Delta\alpha^{(5)}_{\rm had}(M_Z^2)$ as indicated by $\triangledown$. But the tension is at most 1.3σ. c.f. [Crivellin et al, PRL2020].

LQCD does not necessarily show a clear tension to the SM.

Table of Contents

Summary

- **BMW-Nature21:**
  - $a_\mu^{\text{LO-HVP}} = 707.5[5.5] \cdot 10^{-10}$, 0.8% .
  - 1.7σ tension to No New Physics: $718.0[2.8] \times 10^{-10}$.
  - 2.1σ tension to world average of Data-Driven Pheno: $693.1[4.0] \cdot 10^{-10}$.
- **Window Method: Various LQCDs vs. Data-Driven Approach**
  - The latest LQCDs (BMW-20, Mainz-22, ETM-22, RBC/UKQCD-23, FNAL-23) get consistent with 0.6 - 0.7% precision.
  - The LQCDs show more than 3.5σ tension to the latest data-driven approach (Colangelo et al.-22, 0.6% precision).
- **Mainz/CLS: HVP / QED Running Coupling (JHEP-2022):**
  - $\Delta\alpha_{\text{had}}^{(5)}(-5\text{GeV}^2)$ is larger than Data-Driven Pheno w. 2.4σ tension.
  - $\Delta\alpha_{\text{had}}^{(5)}(M_Z^2) = 0.02773(15)$ is consistent with the Data-Driven Pheno and shows 1.3σ tension to EW global fits with $M_{higgs} = 125 GeV$.

Future Works

- LQCDs need per-mil precision consensus for $a_\mu^{\text{LO-HVP}}$ & $\Delta\alpha_{\text{had}}^{(5)}(-Q^2)$.
- Need to specify a source of LQCD-Pheno tensions:
  - Problem in modeling in $\sqrt{s} < 0.7 GeV$ in R-ratio? [Keshavarzi et.al.(2006.12666)].
  - Problem in modeling just after ϕ peak? [Mainz/CLS 2206.06582].
  - More R-ratio data at low energy from Radiative-Return in Belle-II.
  - CMD3 inpact to $a_\mu^{\text{LO-HVP}}$, a_μ^{win}, $\Delta\alpha_{\text{had}}^{(5)}(M_Z^2)$?
- LQCD vs. Data-Driven Phenomenology in the Smeard R-ratio [Hansen et al. PRD2019].
- J-PARC E34 Experiments on Muon g-2 / EDM will bring us to the next stage!

Table of Contents

Continuum Global Fit

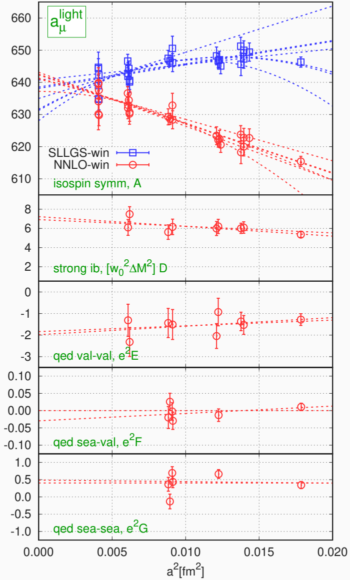

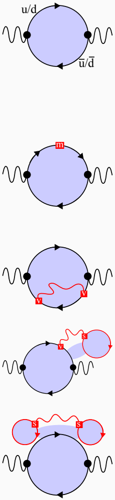

- Model for $a_{\mu,\,ud}^{\text{LO-HVP}}$
  $= A(a^2) + [m_{uds}\ \text{corr.}]$
  $+ D(a^2) \times [\text{SIB corr.}]$
  $+ E(a^2) e_v^2 \leftarrow$ QED valence coupling
  $+ F(a^2)\ e_v e_s$
  $+ G(a^2)\ e_s^2 \leftarrow$ QED sea coupling .
- $A(a^2) = A_0 + A_2 a^2 + A_4 a^4$.
  Similar in $D(a^2)$ & $E(a^2)$.
  No a^4 term in $F(a^2)$ & $G(a^2)$.
- m_{uds} corr. : via $\frac{M_{uu}^2 + M_{dd}^2}{2}$ & M_{ss}^2.
- SIB corr.: via $(M_{dd}^2 - M_{uu}^2)$.

BMW Summary: Quark-Connected QED Corrections

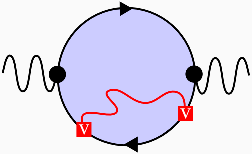

Quark Connected

QED val-val-corr.

$-1.23(40)_{\text{sta}}(31)_{\text{sys}}$

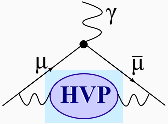

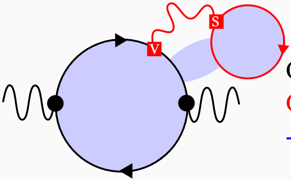

Quark Connected

QED val-sea-corr.

$-0.0093(86)_{\text{sta}}(95)_{\text{sys}}$

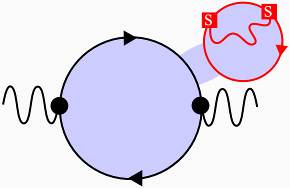

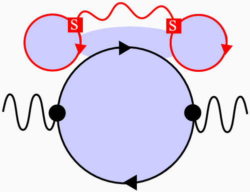

Quark Connected

QED sea-sea-corr.

$0.37(21)_{\text{sta}}(24)_{\text{sys}}$

BMW Summary: Quark-Disconnected QED Corrections

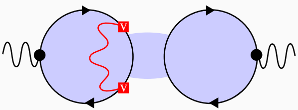

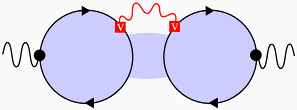

Quark-Disconnected
QED val-val-corr.
$-0.55(15)_{\mathrm{sta}}(10)_{\mathrm{sys}}$

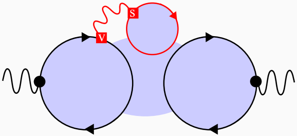

Quark-Disconnected
QED val-sea-corr.
$0.011(24)_{\mathrm{sta}}(14)_{\mathrm{sys}}$

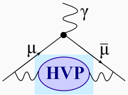

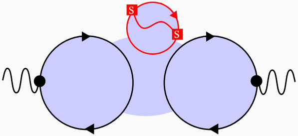

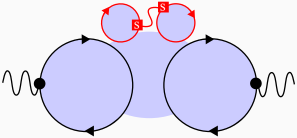

Quark-Disconnected
QED sea-sea-corr.
$-0.040(33)_{\mathrm{sta}}(21)_{\mathrm{sys}}$

BMW Summary: Strong Isospin Breaking Corrections

The strong isospin breaking (SIB) emerges from u/d-quark mass difference:

$$\delta m = m_d - m_u = 2m^0_{ud}\frac{1-r}{1+r}\,, \quad m^0_{ud} := \frac{m_u + m_d}{2}\,, \quad r := \frac{m_u}{m_d} \simeq \frac{m_u^{\overline{MS}}}{m_d^{\overline{MS}}}\,. \tag{26}$$

m^0_{ud} is identified with a light-quark mass in the lattice scheme.

$r = 0.485(20)$ from [BMW-PRL2016].

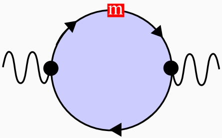

Connected
SIB correction
$6.60(63)_{\rm sta}(53)_{\rm sys}$

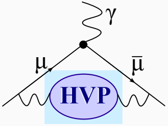

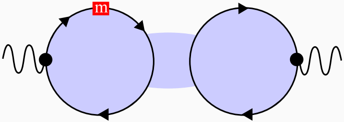

Quark-Disconnected
SIB correction
$-4.67(54)_{\rm sta}(69)_{\rm sys}$

BMW Summary Table for $a_\mu^{\text{LO-HVP}}$

Table: BMW Nature **593** (2021) no.7857.

Observable	Results (10^{-10} units)	Comments
$a_{\mu,\,ud}^{\text{LO-HVP}}$	$639.3(2.0)(4.2)$	with QED/SIB
$a_{\mu,\,s}^{\text{LO-HVP}}$	$53.379(89)(67)$	with QED/SIB
$a_{\mu,\,disc}^{\text{LO-HVP}}$	$-18.61(1.03)(1.17)$	with QED/SIB
$-a_\mu^{1\gamma red}$	-0.321	[FHM-PRD19]
$\Delta^{FV} a_\mu$	$18.7(2.5)$	Simulation/ChPT etc.
$[a_{\mu,\,c}^{\text{LO-HVP}}]_{isosym}$	$14.6(0.0)(0.1)$	[BMW-PRL18]
$[a_{\mu,\,c}^{\text{LO-HVP}}]_{qed}$	$0.0182(36)$	[ETM-PRD19]
$[a_{\mu,\,c}^{\text{LO-HVP}}]_{disc}$	< 0.1	[BMW-PRL18]
$a_{\mu,\,b}^{\text{LO-HVP}}$	$0.271(37)$	[HPQCD-PRD15]
$[a_\mu^{pQCD}]_{\hat{\Pi}(-Q^2>4GeV^2)}$	0.16	[BMW-PRL18]
$a_{\mu,\,tot}^{\text{LO-HVP}}$	$707.5(2.3)_{sta}(5.0)_{sys}[5.5]_{tot}$	0.8% precision

HVP Chiral/Continuum Extrap.

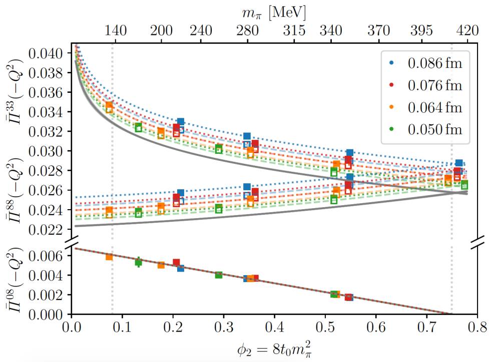

Figure:

- Chiral/Continuum Extrap. at $Q^2 = 1\ GeV^2$. Gray-bands shows continuum limits at a given M_π.
- 33: Isovector (ud). 88 and 08: Isoscalar (uds).

- The chiral/continuum extrapolations of $\Pi(-Q^2)$ are more challenging than the $a_\mu^{\text{LO-HVP}}$ case since the scale $Q \sim \mathcal{O}(1) GeV$ is not well-separated from $\hbar c(\pi/a) \sim 6 - 10 GeV$.
- Idea: At the flavor $SU(3)$ symmetric point ($M_\pi = M_K$), impose $\Pi^{33} = \Pi^{88}$ as a fit constraint.

5f-QED Running Coupling at Z-pole

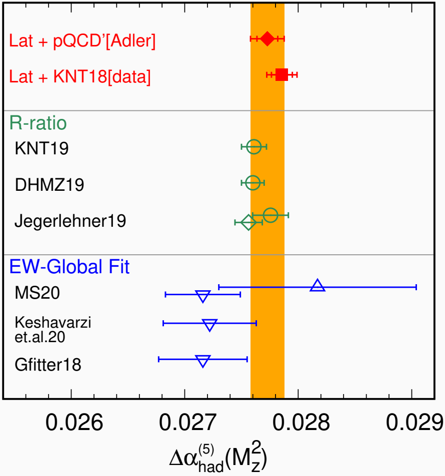

Figure: 5-flavor quark/hadron contributions to QED coupling at Z-pole.